Research Article

Effect of Variation of Magnetic Field Direction on Rayleigh-Taylor Instability in Streaming Dusty Plasma

Meenakshi Yadav [1]*, Harendra Singhal [2], Nagendra Kumar [3]

[1] Department of Mathematics, Gautam Buddha University, Greater Noida, Uttar Pradesh, India

[2] Department of Mathematics, M.M.H. College, Ghaziabad, Uttar Pradesh, India

[3] Department of Mathematics, NIET, Greater Noida, Uttar Pradesh, India

Corresponding Author: * Meenakshi Yadav

DOI: https://doi.org/10.5281/zenodo.21204972

Abstract

We examine the impact of oblique magnetic field on the Rayleigh-Taylor instability (RTI) arising in dusty plasmas. Assuming that dust grains are heavier than ions and electrons, a three-component magnetized dusty plasma is considered. A general dispersion relation is derived to investigate the effect of oblique magnetic field on the Rayleigh-Taylor instability. Variation of growth rates of Rayleigh-Taylor instability with wavenumber are shown graphically for different values of magnetic field inclination with positive y- axis. Rayleigh-Taylor instability is discussed for astrophysical situation near Saturn's E ring in space plasma. It is found that the growth rates of Rayleigh-Taylor instability have linearly increasing pattern in the presence of oblique magnetic field.

Manuscript Information

- **ISSN No:** 2583-7397
- **Received:** 10-05-2026
- **Accepted:** 29-06-2026
- **Published:** 05-07-2026
- **IJCRM:** 5(SP1); 2026: 64-70

- **Plagiarism Checked:** Yes
- **Peer Review Process:** Yes

How to Cite this Article

Yadav M, Singhal H, Kumar N. Effect of Variation of Magnetic Field Direction on Rayleigh-Taylor Instability in Streaming Dusty Plasma. Int J Contemp Res Multidiscip. 2026;5(SP1): 64-70.

Access this Article Online

www.multiarticlesjournal.com

KEYWORDS: Instabilities, Magnetic field, Plasma instability, Rayleigh-Taylor Instability, Dust particles.

1. INTRODUCTION

The dusty plasma is a three-component plasma system consisting of electrons, ions and charged dust grains. The dust grains are usually much heavier than the ions and electrons and get charged by the impact of electrons and ions. However, the charge acquired by the dust grains is influenced not only by the electron and ion currents flowing to its surface but also by various other processes. These include photoelectric emission, secondary emission, and several other factors. Dusty plasma occurs in planetary atmospheres (Musatenko et al. 2006; Tsytovich, 2008) circumstellar clouds, interstellar clouds and in various space environments such as asteroid zones, nebulae, cometary comae, tails and the lower ionosphere of the Earth. When a heavy fluid is supported by a lighter one and gravitational force acts in the direction of decreasing density, the perturbation arising in the plasma becomes unstable. This instability is called Rayleigh-Taylor instability which is observed not only in space environments like the Earth's magnetosphere and the F layer of the ionosphere but also in laboratory plasmas. Rayleigh-Taylor instability and Kelvin-Helmholtz Instability are crucial in shaping astrophysical jets, the region around Saturn's rings, supernova remnants, and various other space plasma phenomena.

D' Angelo (1993) studied the RTI in dusty plasma and found that the presence of negative charged dust substantially reduces the range of unstable wave numbers while the opposite is true for positively charged dust. Sen et al. (2010) and Hoshoudy (2014) studied the RTI in an inhomogeneous dusty plasma in the presence of uniform magnetic field. The Rayleigh-Taylor instability of two superimposed conducting fluids in magnetized un-magnetized plasma has been examined by Sharma and Chhajlani, (1998), and Sharma et al. (2014). Prajapati et al. (2009) have examined the combined RTI and Kelvin-Helmholtz Instability (KHI) in a system of two superimposed magnetized fluids in the presence of suspended dust particles and they found that the magnetic field and particle density have stabilizing influence, while the density difference between the fluids has destabilizing effect on the growth rate of K-H and R-T configurations. Wang et. al. (2010) have explored the combined effects of KHI and RTI with continuous velocity and density profiles, highlighting the linear growth rates. Their findings reveal that the density gradient suppresses the linear growth rate of RTI for short perturbation wavelengths, while the growth rate of KHI increases due to the density gradient but decreases under the influence of the velocity gradient. Several researchers have investigated the growth rate of Rayleigh instability in Hall thrusters. Malik and Singh (2011) examined the influence of temperature on this instability, while Malik et al. (2019) explored the effects of dust accumulation in the exit region of the thruster channel. Verma and Malik (2023) developed a modified Rayleigh-Taylor (RT) instability equation based on a three-fluid Hall thruster plasma model, incorporating multi-ionized ions to examine the growth rate of the RT instability.

In the present study, we examine RTI in an oblique magnetized streaming dusty plasma. It also includes a stability analysis of multilayer dusty fluids with varying magnetic field inclination. The paper is structured as follows. Section 2. presents the formulation of the mathematical model using fundamental equations for electrons, ions, and dusty fluids. In Section 3., analytical dispersion relation for RTI is derived. Results are disused for astrophysical applications near Saturn E ring in section 4. Finally, the results of the study are summarized in Section 5.

2. Governing Equations

We consider the three-component magnetized dusty plasma consisting of ions, electrons and dust grains coupled via downward gravitational acceleration field which acts on the plasma with gravity $\boldsymbol{g} = -g\,\hat{x}$, where $g\,(-g, 0, 0)$ is a constant and $\hat{x}$ is the unit vector along the +ve x- axis. The three components of dusty plasma are coupled via electric field, gravitational acceleration field, and collision forces between the charged species. The dusty plasma is streaming in y-z plane along y direction in the presence of equilibrium magnetic field $\boldsymbol{B}_{d0}$ given by $\boldsymbol{B}_{d0} = (0, B_0 cos\alpha, B_0 sin\alpha)$, where B_0 is constant and α is the angle from positive y axis. A plasma density gradient exists along the positive x- axis and the equilibrium dust density is given by $n_{d0}(x) = \tilde{n}_{d0} e^{\lambda x}$, where λ is taken to be positive constant.

In order to construct basic equations for considered system, we use same model as proposed by Avinash and Sen (2015) as follows

$$0 = -en_e(\boldsymbol{E} + \boldsymbol{u_e} \times \boldsymbol{B}) - \nabla p_e \qquad (1)$$

$$m_i n_i \frac{\partial \boldsymbol{u_i}}{\partial t} = en_i(\boldsymbol{E} + \boldsymbol{u_i} \times \boldsymbol{B}) - \nabla p_i + \mathrm{m_i n_i}\boldsymbol{g} + \boldsymbol{F_i z} \qquad (2)$$

$$m_d n_d \frac{\partial \boldsymbol{u_d}}{\partial t} = -eZ_d n_d(\boldsymbol{E} + \boldsymbol{u_d} \times \boldsymbol{B}) - \nabla p_d + m_d n_d \boldsymbol{g} + \boldsymbol{F_d} \qquad (3)$$

where $m_i, n_{i,}, u_i$ and p_i is the mass, number density, velocity and pressure of the jth (e, i, d) species and Z_d is the number of electrons residing on dust particle, $\boldsymbol{F_{d,i}}$ is the collisional frictional force on the dust particles and ions.

From equations (1), (2) and (3), we get

$$\rho \frac{d\boldsymbol{v}}{dt} = \mathbf{J} \times \mathbf{B} - \nabla p + \rho \boldsymbol{g} \qquad (4)$$

where $\boldsymbol{v} = (m_i n_i \boldsymbol{u_i} + m_d n_d \boldsymbol{u_d})/\rho$, $p = p_e + p_i + p_d$, $\rho = m_i n_i + m_d n_d$ and $\boldsymbol{F_i} + \boldsymbol{F_d} = 0$. The total current density $\boldsymbol{J} = en_i \boldsymbol{u_i} - en_e \boldsymbol{u_e} - eZ_d n_d \boldsymbol{u_d}$ and related to magnetic field $\nabla \times \boldsymbol{B} = 4\pi \boldsymbol{J}$ by Ampere's law. Electric force vanishes due to the neutrality condition $n_i = Z_d n_d + n_{e.}$

The mass conservation equations for ions and dust are given by

$$\frac{\partial n_i}{\partial t} + \nabla \cdot (n_i \boldsymbol{v_i}) = 0, \qquad (5)$$

$$\frac{\partial n_d}{\partial t} + \nabla \cdot (n_d \boldsymbol{v_d}) = 0, \qquad (6)$$

Adding equation (5) and (6), we get

$$\frac{\partial \rho}{\partial t} + \nabla \cdot (\rho \boldsymbol{v}) = 0 \qquad (7)$$

Since ions and electrons are lighter than dust grains, they do not contribute significantly in the momentum transfer and continuity equations, so we assume $\rho \approx m_d n_d \approx \rho_d$ and dust velocity $v = \boldsymbol{v_d}$. Momentum equation and induction equation for dusty magnetized plasma can be written as

$$m_d n_d \frac{\partial v_d}{\partial t} + m_d n_d (\boldsymbol{v}_d \cdot \nabla)\boldsymbol{v}_d + m_d n_d\, \mathbf{g} - \frac{1}{4\pi}(\nabla \times \boldsymbol{B}) \times \boldsymbol{B} + K_B\, T_d \nabla n_d = 0 \qquad (8)$$

$$\frac{\partial \mathbf{B}}{\partial t} = (\boldsymbol{B} \cdot \nabla)\boldsymbol{v}_d - (\boldsymbol{v}_d \cdot \nabla)\boldsymbol{B}, \qquad (9)$$

The above basic equations are linearized assuming that each quantity is represented by the sum of their equilibrium and perturbed parts, as $n_d = n_{d1} + n_{d0}$, $\boldsymbol{v}_d = \boldsymbol{v}_{d1} + \boldsymbol{v}_{d0}$, $\boldsymbol{B} = \boldsymbol{B}_1 + \boldsymbol{B}_0$. The quantities with subscripts "0" and "1" indicate equilibrium and perturbed parts. The perturbation components of dust flow velocity and magnetic field are $\boldsymbol{v}_{d0} = (0,\ v_{0y}, 0)$.
The linearized perturbation equations of the system are as

$$\frac{\partial}{\partial t}\tilde{n}_d + \nabla \cdot \boldsymbol{v_{d1}} + \lambda \hat{x} \cdot \boldsymbol{v_{d1}} + \tilde{n}_d\, \nabla \cdot \boldsymbol{v_{d0}} + \nabla\, \tilde{n}_d \cdot \boldsymbol{v_{0y}} = 0 \qquad (10)$$

$$\frac{\partial \boldsymbol{v_{d1}}}{\partial t} + \boldsymbol{v_{0y}} \cdot \nabla \boldsymbol{v_{d1}} + \tilde{n}_d\, \boldsymbol{g} - \frac{1}{4\pi m_d n_{d0}}\left[\hat{x}\left(\mathrm{B}_0 cos\alpha \frac{\mathrm{d}B_{1x}}{\mathrm{dy}}\right) + \hat{y}\left(-\mathrm{B}_0 sin\alpha \frac{\mathrm{d}B_{1z}}{\mathrm{dy}}\right) + \hat{z}\left(\mathrm{B}_0 cos\alpha \frac{\mathrm{d}B_{1z}}{\mathrm{dy}}\right)\right] + {C_d}^2(\nabla\, \tilde{n}_d + \lambda\, \tilde{n}_d \hat{x}) = 0 \quad (11)$$

$$\frac{\partial \boldsymbol{B_1}}{\partial t} = (\boldsymbol{B}_0 \cdot \nabla)\boldsymbol{v_{d1}} + (\boldsymbol{B}_1 \cdot \nabla)\boldsymbol{v_{0y}} - (\boldsymbol{v_{0y}} \cdot \nabla)\boldsymbol{B_1} - (\mathbf{v_{d1}} \cdot \nabla)\boldsymbol{B_0} \qquad (12)$$

where ${C_d}^2 = \frac{K_B \boldsymbol{T}_d}{m_d}$, $K_B = 1.38 \times 10^{-23} \mathrm{m^2 kg s^{-2} K^{-1}}$ is Boltzmann constant, T_d is temperature of dust particles and m_d is mass of the dust particle.

3. Dispersion relation

A dispersion relation can be obtained by Fourier analysing the first-order perturbed quantities. We assume perturbed quantities varying as $\mathrm{e}^{\mathrm{i}(k_y y + k_z z - \omega t)}$, where k_y and k_z are the wavenumbers in y- and z- directions and ω is the frequency. From equations (10)-(12), we have

$$i\, \lambda v_x - k_y v_y - k_z v_z + \Omega\, \tilde{n}_d = 0 \quad (13)$$

$$\Omega v_x + \mathrm{A}(k_y B_0 cos\alpha + k_z B_0 sin\alpha)B_{1x} + \mathrm{i}(g + \lambda {C_d}^2)\tilde{n}_d = 0 \qquad (14)$$

$$\Omega v_y + \mathrm{A} k_z B_0 sin\alpha B_{1y} - A k_y B_0 sin\alpha B_{1z} - k_y {C_d}^2 \tilde{n}_d = 0 \qquad (15)$$

$$\Omega v_z - \mathrm{A} k_z B_0 cos\alpha B_{1y} + A k_y B_0 cos\alpha B_{1z} - k_z {C_d}^2 \tilde{n}_d = 0 \qquad (16)$$

$$B_{1x} = -\frac{1}{\Omega}\left(k_y B_0 cos\alpha + k_z B_0 sin\alpha\right) v_x \qquad (17)$$

$$B_{1y} = -\frac{1}{\Omega}\left(k_y B_0 cos\alpha + k_z B_0 sin\alpha\right) v_y \qquad (18)$$

$$B_{1z} = -\frac{1}{\Omega}\left(k_y B_0 cos\alpha + k_z B_0 sin\alpha\right) v_z \qquad (19)$$

where $\Omega = \omega - k\boldsymbol{v}_{0y}$ and $A = \frac{1}{4\pi m_d n_{d0}}$.

Using equations (17), (18) and (19) in equations (14), (15) and (16), we obtain

$$(\Omega^2 - AB^2)v_x + i\Omega\left(g + \lambda {C_d}^2\right)\tilde{n}_d = 0 \qquad (20)$$

$$(\Omega^2 - ABk_z B_0 sin\alpha)\, v_y + ABk_y B_0 sin\alpha\, v_z - \Omega k_y {C_d}^2\, \tilde{n}_d = 0 \qquad (21)$$

$$ABk_z B_0 cos\alpha\, v_y + \left(\Omega^2 - ABk_y B_0 cos\alpha\right)v_z - \Omega k_z {C_d}^2\, \tilde{n}_d = 0 \qquad (22)$$

where $B = k_y B_0 cos\alpha + k_z B_0 sin\alpha$.

Equations (13), (20), (21) and (22) can be written in a matrix form as $DX = 0$, where D is a 4× 4 square matrix and X is a 4× 1 column matrix, given by

$$D = \begin{bmatrix} i\lambda & -k_y & -k_z & \Omega \\ \Omega^2 - AB^2 & 0 & 0 & i\Omega\left(g + \lambda {C_d}^2\right) \\ 0 & \Omega^2 - ABk_z B_0 sin\alpha & ABk_y B_0 sin\alpha & -\Omega k_y {C_d}^2 \\ 0 & ABk_z B_0 cos\alpha & \Omega^2 - ABk_y B_0 cos\alpha & -\Omega k_z {C_d}^2 \end{bmatrix}$$

And $X = \begin{bmatrix} v_x \\ v_y \\ v_z \\ \tilde{n}_d \end{bmatrix}$

Non-trivial solution of it can be obtained by putting det. $D = 0$, which gives the following

$$a_1\Omega^6 + a_2\Omega^4 + a_3\Omega^2 + a_4 = 0 \qquad (23)$$

were

$$a_1 = 1$$

$$a_2 = 2AB^2 - \lambda\left(g + \lambda {C_d}^2\right) + k^2 {C_d}^2$$

$$a_3 = -A^2B^4 + AB^2\lambda\left(g + \lambda {C_d}^2\right) - 2AB^2k^2{C_d}^2$$

$$a_4 = A^2B^4k^2{C_d}^2$$

where $k_y = k\, cos\theta, k_z = k\, sin\theta\, , k^2 = k_y^2 + k_z^2$ and θ is the angle between the wave vector $\boldsymbol{k}$ and y- axis.

4. RESULTS AND DISCUSSION

We now perform numerical calculations to determine the growth rate of Rayleigh-Taylor instability (RTI) in space plasma environments near Saturn's E ring. For example, dusty RT structures formed under the influence of gravitational acceleration around the Saturn's E rings. Taking parameters $\lambda \approx 10^{-8}$ m, $g \approx 11\ \mathrm{ms^{-2}}$, ${C_d}^2 \approx 2.28 \times 10^{-9}\ \mathrm{T^{-2}}$, $m_d \approx 7 \times 10^{-10}$ kg, $n_{d0} \approx 15\ cm^{-3}$ and the magnetic field $B_0 = 2.0 \times 10^{-5}$ G. We have shown the variation of growth rate ω_i of Rayleigh-Taylor instability with wavenumber k for different values of $\alpha = \frac{\pi}{6}, \frac{\pi}{4}, \frac{\pi}{3}$ (angle made by magnetic field with positive y-axis) and $\theta = 0, \frac{\pi}{6}, \frac{\pi}{3}, \frac{\pi}{2}$ in figure 1 to 4.

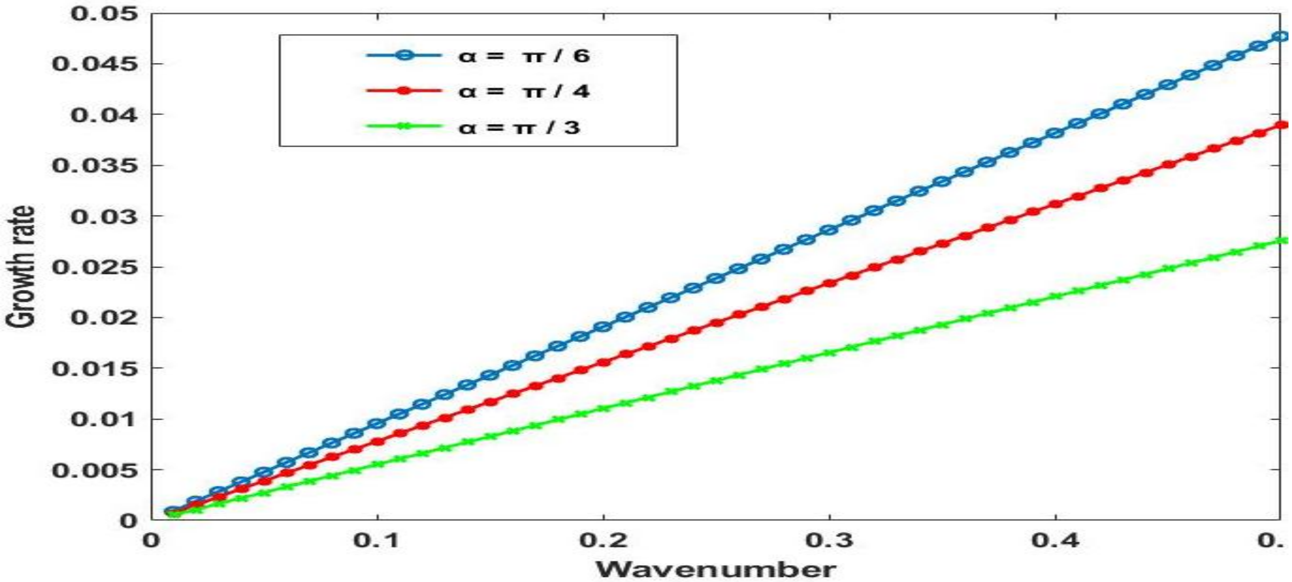

Fig.1: Growth rate ω_i of RTI vs wavenumber k for $v_{0y} = 0.01\ \mathrm{ms}^{-1}$, $\lambda = 10^{-8}$ m, $g = 11\ \mathrm{ms}^{-2}$, ${C_d}^2 = 2.28 \times 10^{-9}\ \mathrm{T}^{-2}$ $m_d = 7 \times 10^{-10}\ kg$, $n_{d0} = 15\ cm^{-3}$, $B_0 = 2.0 \times 10^{-5}$ G, $\alpha = \frac{\pi}{6}, \frac{\pi}{4}, \frac{\pi}{3}$ and $\theta = 0$

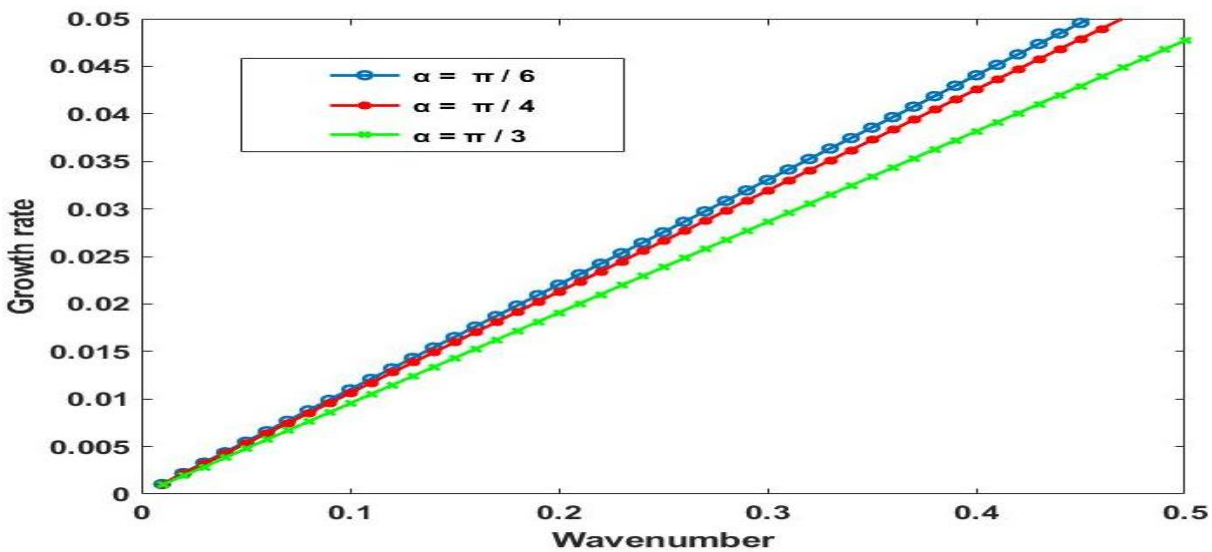

Fig: 2 Growth rate ω_i of RTI vs wavenumber k for $v_{0y} = 0.01\ \mathrm{ms}^{-1}$, $\lambda = 10^{-8}$ m, $g = 11\ \mathrm{ms}^{-2}$, ${C_d}^2 = 2.28 \times 10^{-9}\ \mathrm{T}^{-2}$ $m_d = 7 \times 10^{-10}\ kg$, $n_{d0} = 15\ cm^{-3}$, $B_0 = 2.0 \times 10^{-5}$ G, $\alpha = \frac{\pi}{6}, \frac{\pi}{4}, \frac{\pi}{3}$ and $\theta = \frac{\pi}{6}$

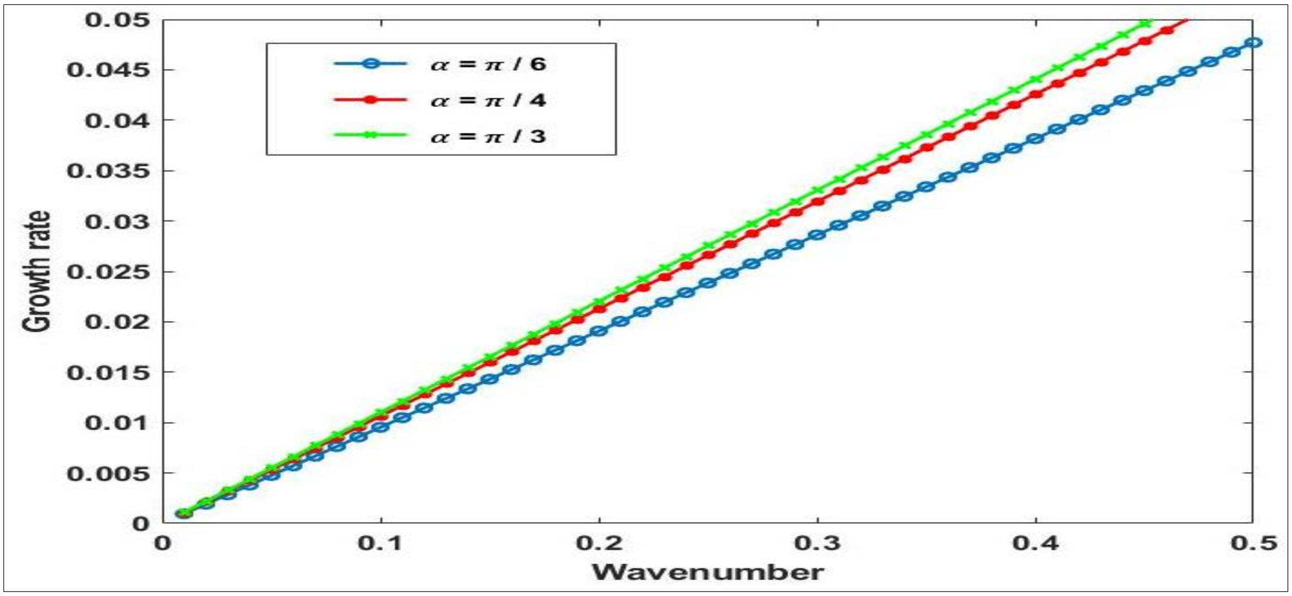

Fig: 3 Growth rate ω_i of RTI vs wavenumber k for $v_{0y} = 0.01\ \mathrm{ms}^{-1}$, $\lambda = 10^{-8}$ m, $g = 11\ \mathrm{ms}^{-2}$, ${C_d}^2 = 2.28 \times 10^{-9}\ \mathrm{T}^{-2}$ $m_d = 7 \times 10^{-10}\ kg$, $n_{d0} = 15\ cm^{-3}$, $B_0 = 2.0 \times 10^{-5}$ G, $\alpha = \frac{\pi}{6}, \frac{\pi}{4}, \frac{\pi}{3}$ and $\theta = \frac{\pi}{3}$

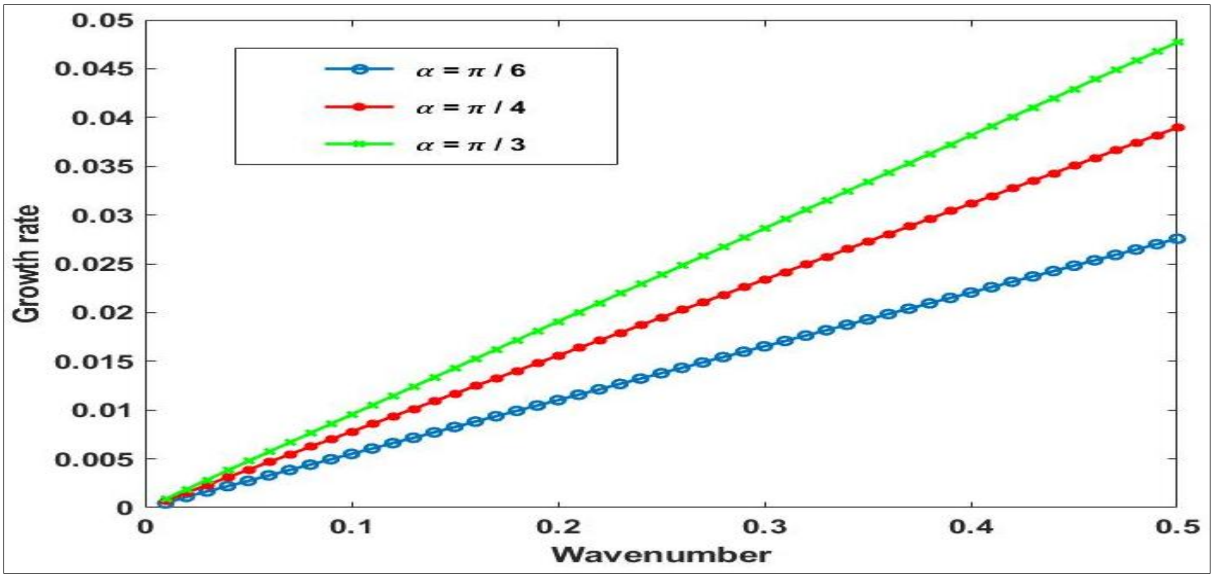

Fig.4. Growth rate ω_i of RTI vs wavenumber k for $v_{0y} = 0.01\ \mathrm{ms}^{-1}$, $\lambda = 10^{-8}$ m, $g = 11\ \mathrm{ms}^{-2}$, ${C_d}^2 = 2.28 \times 10^{-9}\ \mathrm{T}^{-2}$ $m_d = 7 \times 10^{-10}\ kg$, $n_{d0} = 15\ cm^{-3}$, $B_0 = 2.0 \times 10^{-5}$ G, $\alpha = \frac{\pi}{6}, \frac{\pi}{4}, \frac{\pi}{3}$ and $\theta = \frac{\pi}{2}$

Figure 1 shows that the growth rate of instability ω_i increases with the decrease in the inclination of the magnetic field with respect to the positive y axis for $\theta = 0$. For $\theta = \frac{\pi}{6}$, figure 2 depicts a slight increase in the growth rates of instability in comparison to growth rates shown in figure 1 for similar values of α from $\frac{\pi}{3}$ to $\frac{\pi}{6}$. Thus, from Figures 1 and 2, we conclude that the growth rate of instability increases as the magnetic field inclination angle α decreases and θ increases from $\theta = 0$ to

$$\theta = \frac{\pi}{6}.$$

Figure 3 shows that the growth rate of instability ω_i increases with the increase in the values of the magnetic field inclination α for $\theta = \frac{\pi}{3}$. Figure 4 demonstrates that the growth rate of instability also increases with increasing values α for $\theta = \frac{\pi}{2}$. Thus, from figures 3 and 4, it is observed that the growth rate of instability increases with the increases in magnetic field inclination angle α and the decrease in θ from $\frac{\pi}{2}$ to $\frac{\pi}{3}$.

From figures1 and 4, it is observed that the growth rates pattern exhibits a reverse trend when θ changes from $\theta = 0$ to $\theta = \frac{\pi}{6}$. The same behaviour of growth rates is observed in figure 2 for $\theta = \frac{\pi}{3}$ and figure 3 for $\theta = \frac{\pi}{2}$.

5. CONCLUSIONS

In this paper, we have investigated the effect of oblique magnetic field by considering different values of inclination angle of magnetic field on Rayleigh-Taylor Instability. The general dispersion relation is obtained using the normal mode technique. The present study reveals that growth rates of instability of Rayleigh-Taylor instability have linearly increasing behaviour with increasing wavenumber and inclination angle of magnetic field.

It is found that the growth rate of instability increases as the magnetic field inclination angle decreases and θ increases from 0 to $\frac{\pi}{6}$. But, when θ changes from $\frac{\pi}{2}$ to $\frac{\pi}{3}$, the growth rate of instability increases with the increases in magnetic field inclination angle α. It is observed that the growth rates exhibit a reversal pattern when θ changes from 0 to $\frac{\pi}{6}$ and $\frac{\pi}{3}$ to $\frac{\pi}{2}$ .This study might have application in understanding the Rayleigh-Taylor instability in space dusty plasmas, dust outflows near Saturn's E rings and other astrophysical dusty plasma environments.

REFERENCES

1. Musatenko SI, et al. Dusty plasma in the midlatitude ionosphere during meteor showers. Geomagn Aeron. 2006; 46:173.
2. Tsytovich V. *Elementary Processes in Complex Plasma*. Lecture Notes in Physics. Vol. 731. Berlin: Springer; 2008.
3. Avinash K, Sen A. Rayleigh-Taylor instability in a dusty plasma experiment. Phys Plasmas. 2015; 22:083707.
4. Sharma PK, et al. Rayleigh-Taylor instability of two superposed compressible fluids in un-magnetized plasma. In: *Proceedings of the International Conference on Recent Trends in Physics (ICRTP)*; 2014.
5. Prajapati R, et al. Kelvin-Helmholtz and Rayleigh-Taylor instability of two superimposed magnetized fluids with suspended dust particles. Z Naturforsch A. 2009;64A:455-466.
6. Sharma PK, Chhajlani RK. Effect of rotation on the Rayleigh-Taylor instability of two superposed magnetized conducting plasma. Phys Plasmas. 1998;5(6).
7. Sen S, Fukuyama A, Honary F. Rayleigh-Taylor instability in a dusty plasma. J Atmos Sol Terr Phys. 2010; 72:938-942.
8. Hoshoudy GA. Rayleigh-Taylor instability in a dusty plasma. World J Mech. 2014; 4:260-272.
9. Wang LF, Ye WH, Li YJ. Combined effect of the density and velocity gradients in the combination of Kelvin-Helmholtz and Rayleigh-Taylor instabilities. Phys Plasmas. 2010; 17:042103.
10. Verma D, Malik HK. Analytical solution of Rayleigh-Taylor instability in a Hall thruster having double ionized ions. J Theor Appl Phys. 2023;17(5):172353.
11. Malik HK, Sukhmander S. Condition and growth rate of Rayleigh instability in a Hall thruster under the effect of ion temperature. Phys Rev E. 2011; 83:036406.
12. Malik HK, Tyagi J, Sharma D. Growth of Rayleigh instability in a Hall thruster channel having dust in exit region. AIP Adv. 2019; 9:055220.
13. Avinash K, Sen A. Rayleigh-Taylor instability in a dusty plasma experiment. Phys Plasmas. 2015; 22:083707.
14. D'Angelo N. The Rayleigh-Taylor instability in dusty plasmas. Planet Space Sci. 1993;41(6):469-474.